Analysis of the Derivative Coupling Vector for the 1,2 ^{2}A' States of H_3

Seungsuk Han

Department of Chemistry, Myongji University, Yongin, Kyunggi-do 449-728, Korea
Received October 6, 2000

Near the conical intersection for the 1,2 ^{2}A' states of H_3 the derivative coupling vector is calculated and analyzed on the plane of internal coordinates, (U,V) or its polar coordinates (S,θ), based on the squares of the internuclear distances. It is shown that in the vicinity of the conical intersection the derivative coupling vector behaves like $\theta/2S$, which is responsible for the sign changes of the real-valued electronic wave function when the nuclear configuration traverses a closed path enclosing a conical intersection. The analytic property of the wave functions is studied and especially the observation of the sign change in the configuration state function (CSF) coefficients of the real-valued electronic wave functions is demonstrated.

Introduction

In a system with the Jahn-Teller effect[1] two potential energy surfaces exhibit a symmetry-required conical intersection. However the conical intersection is not derived by symmetry. Even in a system, for instance LiNaK, which has no symmetry, the conical intersection may be present.[2] In the vicinity of the conical intersection of adiabatic potential energy surfaces I and J, the nonadiabatic derivative coupling between the two electronic states Ψ_I and Ψ_J,

$$f_{R_\alpha}^{IJ}(\boldsymbol{R}) = \langle \Psi_I(\boldsymbol{r};\boldsymbol{R}) | \frac{\partial}{\partial R_\alpha} \Psi_J(\boldsymbol{r};\boldsymbol{R}) \rangle_r . \quad (1)$$

becomes large near the conical intersection seam. Here the integration is done over the electronic coordinate ($\boldsymbol{r}$) space and $\boldsymbol{R}$ denotes the nuclear coordinate. The standard Born-Oppenheimer treatment[3] breaks down when the nonadiabatic interaction becomes great.

Highly symmetric case like H_3 becomes a simple example to study derivative coupling, since it has a conical intersection seam in equilateral triangle configuration due to the Jahn-Teller effect. The simple system of three hydrogen atoms has one of topological features that introduce a geometric phase, which is related to the derivative coupling. The geometric phase necessitates modification of the standard nuclear Schrödinger equation.[4-8] One would expect the state-to-state cross sections to be particularly sensitive to any phase shifts in the reaction amplitudes for systems, such as $D + H_2 \rightarrow DH + H$. In Adelman *et al.*'s experiments[9] plots of reaction rates versus the final-state rotational quantum number (j) of DH, with H_2 in the ($v = 1, j = 1$) state peaked at a lower value of j than did those of the theoretical calculations[10,11] in which the geometric phase was not included. Kuppermann and Wu[12] explained the discrepancies by the effect of the geometric phase and their calculations also indicate that the differential cross section is far more sensitive than is the total cross section to the inclusion of the geometric phase. Information concerning the existence of conical intersections and/or the behavior of the real-valued electronic wave function along closed loops is required to properly formulate the nuclear dynamics problem.[13]

For the 1,2 ^{2}A' states of H_3 we calculate the derivative coupling vector and analyze it on the plane of internal coordinates based on the squares of the internuclear distances. We obtain the asymptotic form of the derivative coupling vector near the conical intersection, which can be used in dynamics calculation later. We also study the change of the configuration state function (CSF) coefficients of the real-valued electronic wave functions near the conical intersection.

Theoretical Approach, Results and Discussion

Coordinate System. Since we intend to study the geometric properties produced by conical intersection in D_{3h} symmetry of H_3, we follow a suggestion by Mead and Truhlar[4] and employ the same coordinate system which is suitable for our purpose. We deal with internal coordinates based on the squares of the internuclear distances. We use a ring breathing component

$$Q = R_{AB}^2 + R_{BC}^2 + R_{CA}^2 \quad (2)$$

and two components of the E-type vibration

$$U = R_{BC}^2 + R_{CA}^2 - 2R_{AB}^2$$
$$V = \sqrt{3}(R_{BC}^2 - R_{CA}^2). \quad (3)$$

Instead of these coordinates, S and an angle θ, which are defined in terms of the D_{3h} symmetry coordinates U and V, can be used as well: $U = S\cos\theta$, $V = S\sin\theta$ and

$$S^2 = U^2 + V^2$$
$$= 2[(R_{AB}^2 - R_{BC}^2)^2 + (R_{BC}^2 - R_{CA}^2)^2 + (R_{CA}^2 - R_{AB}^2)^2]. \quad (4)$$

Here $S(\equiv sQ)$ is a measure of the deviation from an equilateral triangle configuration ($s = 0$). As shown in Figure 1(a), in the three dimensional space of $(R_{AB}^2, R_{BC}^2, R_{CA}^2)$ the physical region is a cone ($0 \le s \le 1$) due to the triangular relations among the interatomic distances. Cross section of constant Q in the physical region is a circle on the U-V plane as shown in Figure 1(b). Its boundary region ($s = 1$) describes linear configurations of the triatomic molecule.

Consider a molecular configuration such that each atom of H_3 describes a circle of radius e, whose center is at each

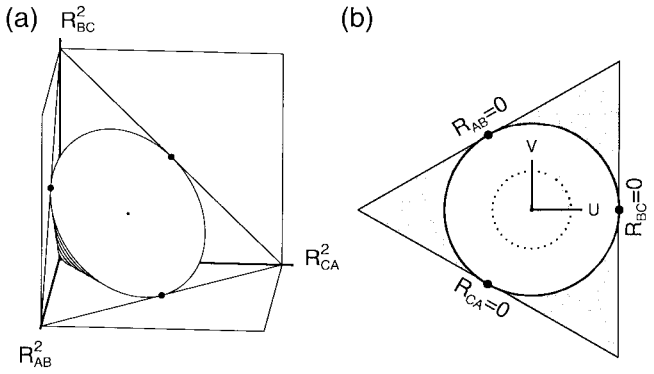

Figure 1. (a) In the space of LEFT (R^2_{AB}, R^2_{BC}, R^2_{CA}) the physical region is a cone. (b) Cross section of constant Q in the physical region is a circle.

equilateral triangular point (with the length of the side $\sqrt{3}\,a$), as shown in Figure 2(a). The circular motions of these atoms are correlated: the vectors of their displacements are shifted in phase through an angle of $4\pi/3$. At any instant of time the equilateral triangle is distorted into an isosceles triangle, and this distortion travels as a wave around the triangle's geometric center, $s = 0$ point in Figure 1(b). Using geometric parameters a, e and θ, the variation of the D_{3h} symmetry coordinates (Q, U, V [S]) for the molecule during the internal rotational motion is given by

$$\begin{aligned} Q &= 9(a^2 + e^2) \\ U &= 18ae\cos\theta \\ V &= 18ae\sin\theta \\ S &= 18ae. \end{aligned} \tag{5}$$

The nuclear configuration performs a rotation along the circle of a radius S on the constant Q plane of Figure 1(b). Figure 2(b) illustrates the derivative coupling vectors which can be determined using an analytic gradient technique.[14] It is interesting to see that the direction of each derivative coupling vector is tangent to each atomic circular displacement described in Figure 2(a), which can be seen by overlapping the two Figures 2(a) and 2(b). The phase obtained from the line integral of the derivative coupling vector along the circular path is increased as the nuclear configuration performs the internal rotation. With the geometric phase this point will

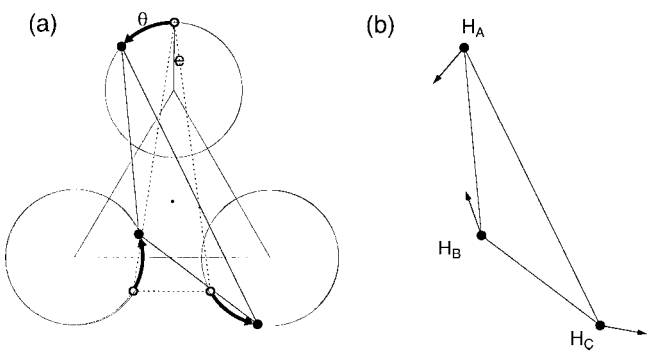

Figure 2. (a) The geometry of the triatomic molecule as a distortion of eqilateral triangle. (b) The derivative coupling vectors evaluated in terms of atom centered displacements.

be explained more in the following section.

Transformed Derivative Coupling. The electronic calculations reported here, 1 ^{2}A' and 2 ^{2}A' potential energy surfaces of H_3 and the 1 ^{2}A'-2 ^{2}A' derivative couplings, are parallel to the work of Yarkony.[13] The adiabatic wave functions and derivative couplings were determined from second order CI wave functions based on a three-electron, three-orbital active space. The molecular orbitals were determined from a complete active space state-averaged multiconfigurational self consistent field procedure in which two ^{2}A' states were averaged with weights (0.505, 0.495) based on (6*s*3*p*1*d*) contracted Gaussian basis sets on the hydrogens. The derivative couplings were determined using an analytic gradient technique.[14]

Yarkony[13] reported the transformed derivative coupling for nuclear configurations [near the lowest energy point on the seam of conical intersection] of a few closed loops enclosing a conical intersection in standard Jacobi coordinates (R, r, γ). Here we extend the work to the whole (Q-constant) U-V plane in the symmetric coordinate system (U, V, Q) and intend to find the limiting formula of the derivative coupling vectors near the conical intersection. The derivative couplings in a H_3 molecule, f_A, f_B and f_C, were evaluated in terms of six atom centered displacements. In the D_{3h} symmetry coordinate system (U, V, Q) which we have chosen, the evaluated couplings are transformed to six parameters f_U, f_V, f_Q, f_ϕ, f_X and f_Y *via* the inverse process of the following transformation:

$$\begin{pmatrix} f_A \\ f_B \\ f_C \end{pmatrix} = \begin{pmatrix} \nabla_A U & \nabla_A V & \nabla_A Q & \nabla_A \phi & \nabla_A X & \nabla_A Y \\ \nabla_B U & \nabla_B V & \nabla_B Q & \nabla_B \phi & \nabla_B X & \nabla_B Y \\ \nabla_C U & \nabla_C V & \nabla_C Q & \nabla_C \phi & \nabla_C X & \nabla_C Y \end{pmatrix} \begin{pmatrix} f_U \\ f_V \\ f_Q \\ f_\phi \\ f_X \\ f_Y \end{pmatrix} \tag{6}$$

where $f_W(\boldsymbol{R}) = \langle \Psi_I(\boldsymbol{r};\boldsymbol{R}) | \frac{\partial}{\partial W} \Psi_J(\boldsymbol{r};\boldsymbol{R}) \rangle_r$ for $W = U, V, Q, \phi, X$ and Y. Here X and Y are the molecular plane components of the vector $(\boldsymbol{R}_A + \boldsymbol{R}_B + \boldsymbol{R}_C)/3$ and ϕ is the rotation angle about the system's center of mass in the molecular plane, $(\phi_A + \phi_B + \phi_C)/3$, so that $\nabla_A \phi = \boldsymbol{z} \times \boldsymbol{R}_A / (3|\boldsymbol{z} \times \boldsymbol{R}_A|^2)$.

Normal and tangential components of the couplings to the circle of a radius S on the U-V plane, (f_S, $(1/S)f_\theta$), are obtained from the transformation of (f_U, f_V) to polar coordinates. In addition to the derivative couplings (f_U, f_V, f_Q) due to the internal (U, V, Q) coordinates, the derivative coupling f_ϕ due to the rotation in the molecular plane is determined. f_θ can also be obtained alternatively from the following equation.

$$\begin{aligned} f_\phi(\boldsymbol{R}) &= \langle \Psi_I(\boldsymbol{r};\boldsymbol{R}) | \frac{\partial}{\partial \phi} \Psi_J(\boldsymbol{r};\boldsymbol{R}) \rangle_r \\ &= \langle \Psi_I(\boldsymbol{r};\boldsymbol{R}) | (\boldsymbol{R}_A \times \nabla_A + \boldsymbol{R}_B \times \nabla_B + \boldsymbol{R}_B \times \nabla_B) | \Psi_J(\boldsymbol{r};\boldsymbol{R}) \rangle_r \\ &= \boldsymbol{R}_A \times \boldsymbol{f}_A + \boldsymbol{R}_B \times \boldsymbol{f}_B + \boldsymbol{R}_C \times \boldsymbol{f}_C \end{aligned} \tag{7}$$

which were confirmed by taking the inverse of the transfor-

mation matrix in Eq. (6) using a symbolic mathematical program Maple. The coupling f_θ is a transformation property of a system under rotations of the *nuclear* system only, which is not the total system [nuclei + electrons]. It follows that the commutators of L_z^e and L_z^n (the z component of total electron and nuclear angular momentum operators, respectively) with the electronic hamiltonian have the relation

$$[L_z^e, H^e(\boldsymbol{r};\boldsymbol{R})] = -[L_z^n, H^e(\boldsymbol{r};\boldsymbol{R})] \tag{8}$$

and thus

$$\langle \Psi_I(\boldsymbol{r};\boldsymbol{R})\left|L_z^e\right|\Psi_J(\boldsymbol{r};\boldsymbol{R})\rangle_r = -\langle \Psi_I(\boldsymbol{r};\boldsymbol{R})\left|L_z^n\right|\Psi_J(\boldsymbol{r};\boldsymbol{R})\rangle_r . \tag{9}$$

Therefore the magnitude of coupling f_ϕ must equal the interstate matrix element of L_z^e. Since the evaluation of the matrix element does not involve the analytic gradient technique, the equivalence of the two approaches provides a measure of the precision of the derivative couplings. In the work of Yarkony,[13] whose method we employ in the computation of energy and derivative coupling, it was reported that the two approaches agree to 1×10^{-6}. Here we are not interested in f_X and f_Y which may have a similar transformation property of a system under translation of the nuclear system only.

Due to D_{3h} symmetry in a H_3 molecule, all the transformed coupling values are oscillating with the period of $2\pi/3$ as the nuclear configuration traverses along the circle of a constant S on U-V plane. Since the nuclear configuration of $\theta = 0$ is an isosceles triangle as in Figure 2(a), E_2–E_1, f_θ and f_ϕ [Sf_S and f_Q] are even [odd] functions of θ and they can be expanded in Fourier cosine [sine] series of period $2\pi/3$:

$$f^e(s, \theta) = \sum_{n=0}^{\infty} C_{3n}(s)\cos(3n\theta)$$

$$f^o(s, \theta) = \sum_{n=1}^{\infty} C_{3n}(s)\sin(3n\theta). \tag{10}$$

In a constant-Q plane, where the equilateral triangle configuration with the side of $R(\text{H–H}) = 4.55901a_0$ has the degenerate electronic energy $E_1 = E_2 = -1.504951$ hartree, the Fourier coefficients of energy difference and the transformed couplings, $C_{3n}(s)[S_{3n}(s)]$, are tabulated for various s in Tables 1-4.

When transported along a closed loop enclosing a conical intersection, the sign changes of the real-valued electronic wave function result from the geometry dependent phase factor in the electronic wave function, $\exp(-i\oint \sum_\alpha \boldsymbol{f}_\alpha \cdot d\boldsymbol{R}_\alpha)$. Since H_3 molecule has a conical intersection seam in the equilateral triangle configuration, it is noted that for a circle of radius S on the U-V plane the circulation of derivative coupling vectors along the path gives the geometric phase π, that is

$$\oint \sum_\alpha \boldsymbol{f}_\alpha \cdot d\boldsymbol{R}_\alpha = \oint [\boldsymbol{f}_A \cdot d\boldsymbol{R}_A + \boldsymbol{f}_B \cdot d\boldsymbol{R}_B + \boldsymbol{f}_C \cdot d\boldsymbol{R}_C]$$
$$= \int_0^{2\pi} f_\theta d\theta = \pi \tag{11}$$

which is contributed only from the coefficient $C_0(s)$[=0.5] of

Table 1. Fourier coefficients of E_2-E_1, the energy difference between 1 ^{2}A' and 2 ^{2}A' potential energy surfaces of H_3, for various s

n	s	E_2–E_1					
		C_0	C_3	C_6	C_9	C_{12}	C_{15}
1	0.00174533	0.0000907	-0.0000001				
2	0.00349065	0.0001813	-0.0000006				
3	0.00523596	0.0002719	-0.0000013				
4	0.00698126	0.0003626	-0.0000024				
5	0.00872654	0.0004532	-0.0000037				
6	0.01047178	0.0005439	-0.0000054				
7	0.01221700	0.0006346	-0.0000073				
8	0.01396218	0.0007253	-0.0000096				
9	0.01570732	0.0008161	-0.0000121				
10	0.01745241	0.0009068	-0.0000150	-0.0000001			
11	0.03489950	0.0018169	-0.0000599	-0.0000005			
12	0.05233596	0.0027335	-0.0001351	-0.0000017			
13	0.06975647	0.0036598	-0.0002410	-0.0000039	-0.0000001		
14	0.08715574	0.0045993	-0.0003780	-0.0000076	-0.0000003		
15	0.10452846	0.0055551	-0.0005468	-0.0000132	-0.0000007		
16	0.12186934	0.0065307	-0.0007484	-0.0000208	-0.0000012	-0.0000001	
17	0.13917310	0.0075294	-0.0009836	-0.0000309	-0.0000020	-0.0000002	
18	0.15643447	0.0085546	-0.0012538	-0.0000437	-0.0000032	-0.0000003	
19	0.17364818	0.0096098	-0.0015602	-0.0000596	-0.0000049	-0.0000005	-0.0000001
20	0.34202014	0.0226013	-0.0070237	-0.0004281	-0.0000694	-0.0000133	-0.0000030
21	0.50000000	0.0427320	-0.0187582	-0.0011862	-0.0002965	-0.0000789	-0.0000252
22	0.64278761	0.0740009	-0.0405568	-0.0019575	-0.0007743	-0.0002470	-0.0000985
23	0.76604444	0.1197297	-0.0770070	-0.0015297	-0.0016047	-0.0005311	-0.0002497
24	0.86602540	0.1802027	-0.1310965	0.0022964	-0.0031173	-0.0007804	-0.0005256

Table 2. Fourier coefficients of f_θ , the 1 ^{2}A'-2 ^{2}A' derivative couplings of H_3 for various s

n	f_θ					
	C_0	C_3	C_6	C_9	C_{12}	C_{15}
1	0.500000	0.002476	0.000004			
2	0.500000	0.004952	0.000016			
3	0.500000	0.007427	0.000037			
4	0.500000	0.009903	0.000065			
5	0.500000	0.012378	0.000102	0.000001		
6	0.500000	0.014853	0.000147	0.000001		
7	0.500000	0.017328	0.000200	0.000002		
8	0.500000	0.019803	0.000261	0.000003		
9	0.500000	0.022277	0.000331	0.000005		
10	0.500000	0.024751	0.000408	0.000007		
11	0.500000	0.049457	0.001631	0.000054	0.000002	
12	0.500000	0.074077	0.003662	0.000181	0.000009	
13	0.500000	0.098567	0.006489	0.000427	0.000028	0.000002
14	0.500000	0.122885	0.010096	0.000828	0.000068	0.000006
15	0.50000	0.146993	0.014463	0.001420	0.000139	0.000014
16	0.50000	0.170851	0.019568	0.002235	0.000255	0.000030
17	0.50000	0.194422	0.025381	0.003302	0.000430	0.000057
18	0.5000	0.217673	0.031874	0.004647	0.000678	0.000101
19	0.5000	0.240572	0.039012	0.006292	0.001015	0.000168

Table 3. Fourier coefficients of Sf_S

n	Sf_S				
	S_3	S_6	S_9	S_{12}	S_{15}
1	0.000825	-0.000001			
2	0.001651	-0.000005			
3	0.002476	-0.000012			
4	0.003301	-0.000022			
5	0.004125	-0.000034			
6	0.004950	-0.000049	-0.000001		
7	0.005774	-0.000067	-0.000001		
8	0.006599	-0.000087	-0.000001		
9	0.007423	-0.000110	-0.000002		
10	0.008246	-0.000136	-0.000002		
11	0.016453	-0.000543	-0.000018	-0.000001	
12	0.024584	-0.001217	-0.000060	-0.000003	
13	0.032601	-0.002150	-0.000141	-0.000009	-0.000001
14	0.040469	-0.003334	-0.000274	-0.000022	-0.000002
15	0.048154	-0.004758	-0.000467	-0.000046	-0.000004
16	0.055625	-0.006406	-0.000732	-0.000084	-0.000009
17	0.062853	-0.008265	-0.001075	-0.000140	-0.000018
18	0.069814	-0.010316	-0.001504	-0.000219	-0.000031
19	0.076484	-0.012543	-0.002023	-0.000326	-0.000051

f_θ in Table 2. The phase can also be obtained directly from the derivative coupling vectors before the coordinate transformation as long as we find the geometric parameters a, e and θ *via* Eqs. (2), (3) and (5). For a geometry in the middle of the internal rotational motion shown in Figure 2(a) the calculated derivative coupling vectors may be displayed as in Figure 2(b). Generally the direction of each derivative coupling vector, f_A, f_B and f_C, tends to be tangent to each atomic circular displacement of radius e. The norm of each coupling vector is about $e/6$ so that the complete line integral in Eq. (11) can give the phase value π. Eq. (11) is satisfied for *any* closed loop, not just in the infinitesimal vicinity of the conical intersection as long as the loop encloses a conical intersection seam.

Table 4. Fourier coefficients of f_Q and f_θ

n	f_Q				f_θ	
	S_3	S_6	S_9	S_{12}	C_0	C_3
1	0.000004				0.055011	
2	0.000008				0.055011	
3	0.000012				0.055011	
4	0.000016				0.055011	
5	0.000019				0.055011	
6	0.000023				0.055011	
7	0.000027				0.055010	
8	0.000031				0.055010	
9	0.000035	0.000001			0.055009	
10	0.000039	0.000001			0.055009	
11	0.000078	0.000003			0.055001	
12	0.000116	0.000006			0.054989	0.000001
13	0.000154	0.000010	0.000001		0.054971	0.000002
14	0.000191	0.000016	0.000001		0.054948	0.000003
15	0.000227	0.000022	0.000002		0.054920	0.000005
16	0.000262	0.000030	0.000003		0.054885	0.000009
17	0.000296	0.000039	0.000005	0.000001	0.054844	0.000013
18	0.000328	0.000049	0.000007	0.000001	0.054797	0.000018
19	0.000359	0.000059	0.000010	0.000002	0.054743	0.000024

Especially in the vicinity of the conical intersection, as a consequence of $\lim_{S\to 0} f_\theta = 1/2$ and $\lim_{S\to 0} Sf_S = 0$ in Tables 2 and 3, it follows that the derivative coupling vector in the U-V plane behaves like

$$\lim_{S\to 0} \boldsymbol{f}(S, \theta) = \frac{\boldsymbol{\theta}}{2S} \tag{12}$$

where $\boldsymbol{\theta}$ is the unit vector in the direction of increasing azimuthal angle. The directions of the coupling vectors on the U-V plane are tangent to the circle of a radius S as shown in Figure 3. The definite sign in Eq. (12) is immaterial because of an arbitrary choice in the signs of the electronic wave functions $\Psi_I(\boldsymbol{r}; \boldsymbol{R})$ and $\Psi_J(\boldsymbol{r}; \boldsymbol{R})$ in Eq. (1). The circulating behavior of the coupling vector is responsible for the sign change of the involved electronic wave functions after one turn around the intersection point in the nuclear configuration space. If system is transported along a straight path C on the U-V plane in Figure 3 the component of the derivative coupling to the moving direction has the Lorentzian shape:

$$f_a(b) = \frac{a/2}{a^2 + b^2} \tag{13}$$

where a denotes the closest distance to the conical intersection seam in the path and b denotes a perpendicular displacement from the closest point. The derivative coupling also

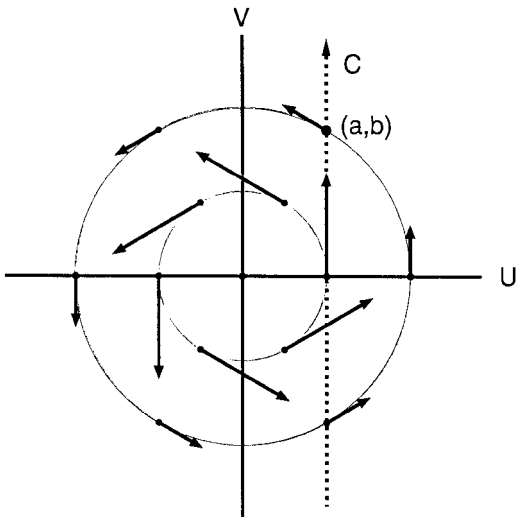

Figure 3. The derivative coupling vectors on the *U-V* plane in the vicinity of the conical intersection.

displays the Lorentzian shape near avoid crossing region of potential energy curves for diatomic molecules.

CSF Coefficients in Electronic Wave Functions. Concerning the presence of conical intersections, we may also examine the behavior of the electronic wave functions along closed loops without calculating the derivative coupling vectors. Rudenberg[15,16] pointed out the possibility that information about the presence of conical intersections may be found out from the configuration state function (CSF) coefficients of the real-valued electronic wave functions.

In this section we concentrate on the variation of the CSF coefficients along a closed loop in a lower level calculation for the 1,2 $^2A'$ states of H_3 which has a conical intersection seam in D_{3h} symmetry. The wave functions were obtained from state-averaged multiconfiguration self-consistent field (SA-MCSCF) calculations using the GAMESS program[17] in the full valence space consisting of 240 CSFs in C_s. The two states were averaged with equal weights. We calculated 1,2 $^2A'$ states at 36 consecutive points around the circular loop outlined by the points in Figure 1(b). The energy differences between 1,2 $^2A'$ states for the configurations in the chosen loop is about 5.8 mhartree. The variation of the CSF coefficients of the dominant electron configurations in the wave functions were monitored. All the optimized orbitals remain almost the *same* as the nuclear configuration changes, so that we need to examine the variation of CSF coefficients for any change in the 1 $^2A'$ and 2 $^2A'$ states.

Figure 4 displays the variation of three dominant CSF coefficients, CSFs [210, 201, 111], for 1 $^2A'$ and 2 $^2A'$ states of H_3 as the molecular geometry changes along the circular path. The lowest energy orbital has D_{3h} symmetry and the second and third ones have single nodes perpendicular to each other. *All CSF coefficients vary smoothly like sinusoidal functions and change sign after one revolution*, which results from the presence of a conical intersection seam inside the loop. This method can be used to check whether there exists a conical intersection seam inside a chosen loop.

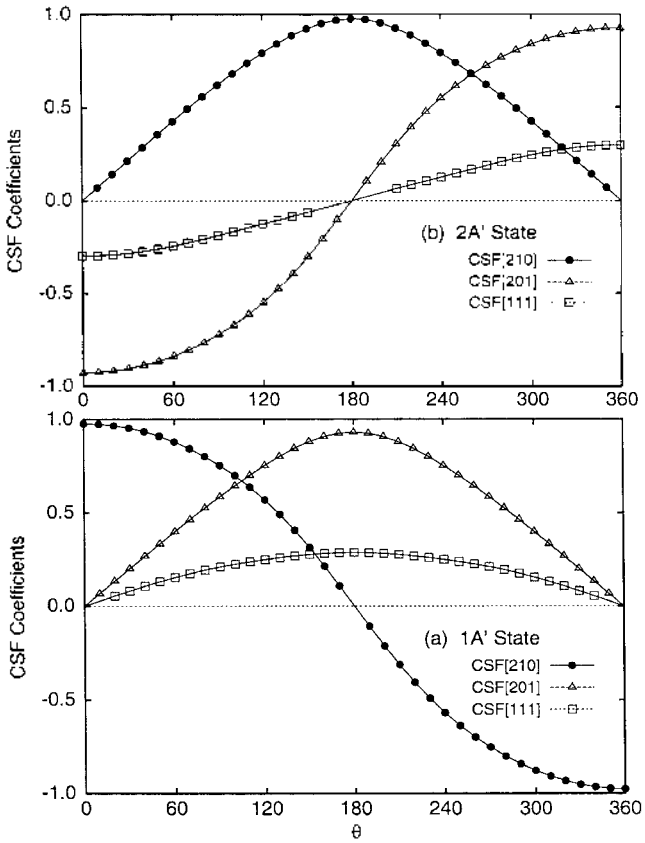

Figure 4. The dominant CSF coefficients for (a) 1 $^2A'$ and (b) 2 $^2A'$ states of H_3 as a function of the geometric parameter θ.

Comparing Figures 4(a) and 4(b), it is noticed that the phases of the CSF coefficients for 2 $^2A'$ state are shifted by π from those for 1 $^2A'$ state. Therefore it can be said that the upper electronic state of geometric phase θ is analytically close to the lower state of phase $\theta - \pi$ rather than θ. The upper electronic state of phase θ can be obtained from the lower electronic state of phase $\theta - \pi$ by analytic continuation moving through (rather than going around) the conical intersection point to the opposite position in the nuclear configuration space. This fact agrees to the mention of Blais *et al.*[18] that the two surfaces having a conical intersection may be considered as two Riemann sheets of the same analytic function.

Acknowledgment. The author thanks D. R. Yarkony for this work. This work was supported by grant No. 1999-2-121-005-3 from the interdisciplinary Research program of the KOSEF.

References

1. Jahn, H. A.; Teller, E. *Proc. R. Soc. London, Ser. A* **1937**, *161*, 220.
2. Varandas, J. C.; Tennyson, J.; Murrel, J. N. *Chem. Phys. Lett.* **1979**, *61*, 431.
3. Born, M.; Oppenheimer, J. R. *Ann. Phys. (N. Y.)* **1927**, *84*, 457.
4. Mead, C. A.; Truhlar, D. G. *J. Chem. Phys.* **1979**, *70*, 2284.

5. Mead, C. A. *Chem. Phys.* **1980**, *49*, 23.
6. Kendrick, B.; Pack, R. T. *J. Chem. Phys.* **1996**, *104*, 7475.
7. Kendrick, B.; Pack, R. T. *J. Chem. Phys.* **1996**, *104*, 7502.
8. Yarkony, D. R. *Rev. Mod. Phys.* **1996**, *68*, 985.
9. Adelman, D. E.; Shafer, N. E.; Kliner, D. A. V.; Zare, R. N. *J. Chem. Phys.* **1992**, *97*, 7323.
10. Mielke, S. L.; Friedman, R. S.; Truhlar, D. G.; Schwenke, D. W. *Chem. Phys. Lett.* **1992**, *188*, 359.
11. Neuhauser, D.; Judson, R. S.; Kouri, D. J.; Adelman, D. E.; Shafer, N. E.; Kliner, D. A. V.; Zare, R. N. *Science* **1992**, *257*, 519.
12. Kuppermann, A.; Wu, Y.-S. M. *Chem. Phys. Lett.* **1993**, *205*, 577.
13. Yarkony, D. R. *J. Chem. Phys.* **1996**, *105*, 10456.
14. Lengsfield, B. H.; Yarkony, D. R. In *State-Selected and State to State Ion-Molecule Reaction Dynamics: Part 2 Theory*; Baer, M., Ng, C.-Y., Eds.; Wiley: New York, U. S. A., 1992; Vol. 82.
15. Xantheas, S.; Elbert, S. T.; Ruedenberg, K. *J. Chem. Phys.* **1990**, *93*, 7519.
16. Xantheas, S. S.; Atchity, G. J.; Elbert, S. T.; Ruedenberg, K. *J. Chem. Phys.* **1991**, *94*, 8054.
17. Schmidt, M. W.; Baldridge, K. K.; Boatz, J. A.; Elbert, S. T.; Gordon, M. S.; Jensen, J. J.; Koseko, S.; Matsunaga, N.; Nguyen, K. A.; Su, S.; Windus, T. L.; Dupuis, M.; Montgomery, J. A. *J. Comput. Chem.* **1993**, *14*, 1347.
18. Blais, N. C.; Truhlar, D. G.; Mead, C. A. *J. Chem. Phys.* **1988**, *89*, 6204.